DEVELOPMENT OF AN ALGORITHM BASED ON DEEP LEARNING FOR THE CLASSIFICATION OF GEOPHYSICAL PHENOMENA FROM THE TENGEOP-SARWV SAR IMAGE DATABASE

Lucas Taipe, Sergio Sosa, Omar Blas

ABSTRACT

Synthetic aperture radar data have multiple applications when we use Deep Learning algorithms. In this paper we design a neural network to classify marine geophysical phenomena to complement data taken directly at the survey site. The data from the TenGeoP-SARwv dataset will be taken 5500 to be used in the neural network where 2310 are for training, the data train will be increased by image transformations, the new data train is 6930. The NSCNNMGeophysical neural network will be used for training and validation. We obtained the performance metrics of the neural network model which gives us a representation of the results that would be obtained by testing an image. The proposed neural network proved to be reliable when evaluated with the proposed performance metrics in the radar competition using little training data.

***Index Terms*—** Neural networks, Deep learning, SAR images, Geophysical phenomena.

1. INTRODUCTION

Synthetic Aperture Radar (SAR) systems are used to process the information captured by an antenna using algorithms; these databases collected by satellites have applications in agriculture for mapping and monitoring of soil and crop characteristics, soil tillage, crop residue mapping and moisture estimation [1]; Furthermore, satellite data can be used for the study of subsidence due to aquifer exploitation, deformations are calculated based on the relative displacement between two bodies, inclinations and movements in depth [2]. The estimation of flooded areas to help understand hydrological conditions, surface water availability and prevent natural disasters [3]. Another application is oil spill monitoring using supervised learning algorithms such as Support vector machine (SVM) [4], with these methods it is possible to obtain images of the expansion of oil in the sea. The data that will be used from sentinel-1 SAR in Wave Mode (WV) will allow to determine the direction and height of the waves in the ocean with images of 20x20km resolution [5] with the purpose of using a deep learning process to track tree felling in the Amazon rainforest [6].

Currently, remote sensing with SAR images help to meet the goals of the Sustainable Development Goals (SDGs) set by the United Nations (UN) [8]; in this way we understand the geophysical phenomena of the ocean and can take better measures against environmental disasters caused by companies in the ocean. Especially, targets 9.1, 9.4, 9.5, 9.a, 14.2, 14.a of SDG 9 industry, innovation and infrastructure and SDG 14 underwater life are related to economic activities in the ocean that directly affect marine ecosystems and fishing communities. Indicators 9.1.1 and 9.4.1 of the targets can be obtained with SAR imagery [9] through the TenGeoP-SARwv dataset.

The dataset used will be TenGeoP-SARwv whose database is obtained from Sentinel-1A satellite in VV polarization. Labeled images of geophysical phenomena (pure sea waves, wind gusts, convective microcells, rain cells, rain cells, biological slices, sea ice, iceberg, low wind area, atmospheric front, ocean front) can be obtained with these data [7].

In this paper an efficient neural network is proposed for the classification of the TenGeoP-SARwv database, with images from this database a database composed of less than 15% of initial data was built, this new database went through a clustering process for training, validation and test data to be used in the training of the proposed neural network. The efficiency of the neural network will be evaluated with performance metrics such as precision, recall, accuracy, F-1 score, confusion matrix and ROC curves.

2. METHODOLOGY

2.1. Red neuronal NSCNNMGeophysical

We define the architecture of the NSCNNMGeophysical neural network using the following algorithm.

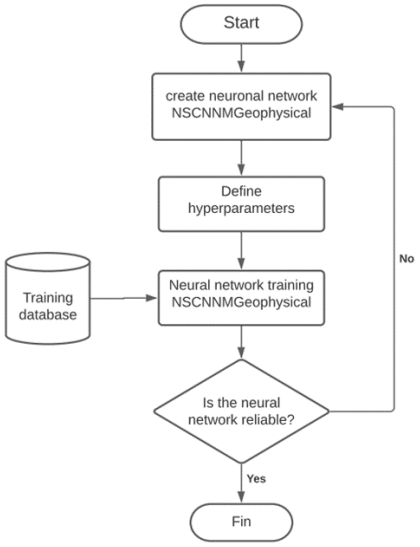

Figure 1: Algorithm for training the NSCNNMGeophysical neural network.

2.2. Data collection

The TenGeoP-SARwv dataset is established based on S-1A WV acquisitions in VV polarization. this dataset consists of 37. 553 SAR vignettes divided into our ten physical geo-categories: Pure ocean waves (POW), Wind streaks (WS), Micro convective cells (MCC), Rain cells (RC), Biological slicks (BS), Sea ice (SI), Iceberg (IB), Low wind areas (LWA), Atmospheric front (AF) and Oceanic front (OF). SAR selection images cover the full year of 2016 and are manually labeled by visual inspection following criteria documented in [10].

Table 1: SAR image numbers of the labelled dataset for each class in every month of 2016. [10]

	Jan	Feb	Mar	Apr	May	Jun	Jul	Aug	Sep	Oct	Nov	Dec	Total
POW	406	407	408	409	406	408	410	409	409	409	408	411	4,900
WS	406	409	403	407	404	391	396	398	397	398	384	404	4,797
MCC	396	384	370	384	385	365	386	388	380	391	384	385	4,598
RC	398	399	398	395	398	391	395	393	393	396	394	390	4,740
BS	398	394	395	398	397	339	397	398	397	400	398	398	4,709
SI	387	150	282	396	396	392	393	393	396	396	396	393	4,370
IB	399	417	308	146	58	29	10	14	12	29	159	399	1,980
LWA	137	137	138	220	201	95	214	144	207	207	241	219	2,160
AF	360	282	301	348	363	234	361	377	378	367	364	365	4,100
OF	61	85	64	102	131	60	116	135	96	108	132	109	1,199
Total	3,348	3,064	3,067	3,205	3,139	2,704	3,078	3,049	3,065	3,101	3,260	3,473	37,553

2.2. Data preparation

From the TenGeoP-SARwv database we randomly extracted 550 images for each class, resizing each image to a size of 300x300 pxs, in this way we will obtain a new database whose number of images represents 14.65 % of the TenGeoP-SARwv database and without losing the characteristics of each class.

The new database will be composed of 5500 images, for the training of the neural network the database will be divided into 70% and 30% for training and test respectively; then the training data will be divided into 60% and 40% for training and validation, being distributed as shown in Table 2.

Table 2: Distribution of images.

Size	Training	Validation	Test	Total
300x300x3	2310	1540	1650	5500

Due to the small amount of images per class we will use the data augmentation to improve our database, using the ImageDataGenerator function of Keras we will apply transformations obtaining 2 images for each image of the database, achieving a more robust database.

Table 3: Distribution of images with magnification.

Size	Training	Validation	Test	Total
300x300x3	6930	1540	1650	10120

The transformations applied to the database were *vertical_flip*, *horizontal_flip* and *zoom_range*, taking into account that each magnified image faithfully represents the distinctive characteristics of each class.

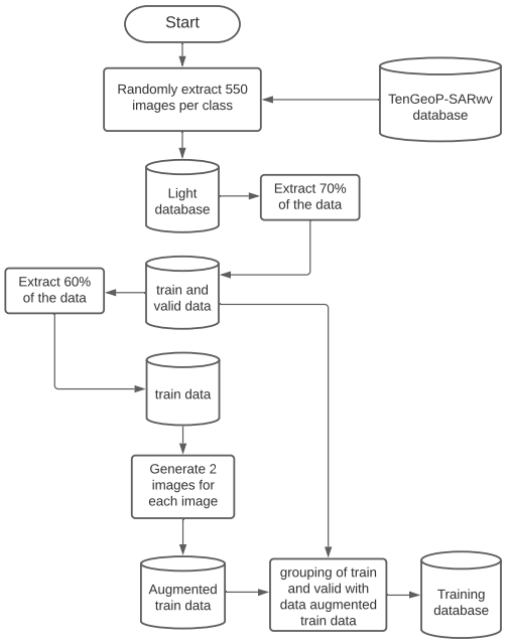

Figure 2: Schematic of image extraction from the TenGeoP-SARwv database, Source: Research Image.

2.3 NSCNNMGeophysical neural network architecture

The NSCNNNMGeophysical neural network is composed of convolution and maximum clustering layers in a non-sequential manner, the distribution of the layers and their characteristics can be found in Table 3 and the general representation of the network structure is shown in Figure 3.

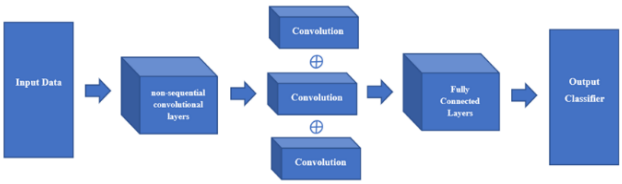

Figure 3: An overview of the proposed NSCNNM - Geophysical architecture, Source: Research Image.

Table 4: Architecture of the NSCNNNMGeophysical neural network, Source: Research Imaging.

Layer	Layer type	Size	N°weight	N° of file	Output	Connected
Input					300x300x3	
Layer 1	Conv	7x7	9472	64	64x294x294	Input
Layer 2	Max-pool	3x3			64x98x98	Layer1
Layer 3	Conv	3x3	73856	128	128x96x96	Layer2
Layer 4	Max-pool	3x3			128x32x32	Layer3
Layer 5	Conv	2x2	65664	128	128x32x32	Layer4
Layer 6(Add)	Max-pool	2x2			128x32x32	Layer5 and Layer4
Layer 7	Conv	3x3	147584	128	128x32x32	Layer6(Add)
Layer 8(Add)	Max-pool	3x3			128x32x32	Layer6 and Layer7
Layer 9	Conv	3x3	221376	192	192x30x30	Layer(Add)
Layer 10	Max-pool	7x7			192x4x4	Layer9
Layer 11-1	Conv	3x3	442624	256	256x4x4	Layer10
Layer 11-2	Conv	3x3	442624	256	256x4x4	Layer10
Layer 11-3	Conv	3x3	442624	256	256x4x4	Layer10
Layer 12-1	Max-pool	3x3			256x1x1	Layer11-1
Layer 12-2	Max-pool	3x3			256x1x1	Layer11-2
Layer 12-3	Max-pool	3x3			256x1x1	Layer11-3
Concatenate						
Layer 13	Flatten				768	Concatenate
Layer 14	Dense		98432		512	Layer 13
Dropout 1	Dropout				512	Layer 14
Layer 16	Dense		-		128	Layer 15
Dropout 1	Dropout				128	Layer 16
Layer 18	Dense		1290		10	Layer 17
Total params: 1 945 546						
Trainable params: 1 945 546						
Non-trainable params: 0						

2.4 Model training

The values defined for the hyperparameters in the training were 40 epochs, a batch size of 64, ADAM stochastic gradient descent optimizer, Relu activation function for the hidden layers and for the final classification layer a softmax activation function was used; and as loss function the categorical_crossentropy method.

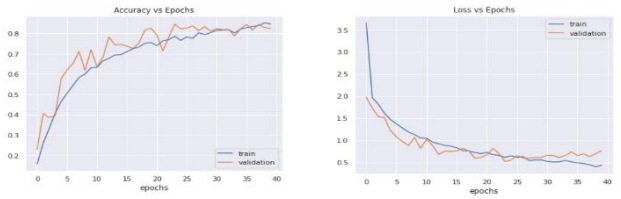

(a) (b)

Figure 4: Training of the NSCNNMGeophysical model. (a) Graph of accuracy as a function of each training epoch. (b) Loss plot as a function of each training epoch. Source: Research Imagino.

For the training of the NSCNNMGeophysical neural network, the google colab platform with nvidia-tesla-v100-32gb gpu was used.

2.4 Performance evaluation

The performance metrics of the neural network model will be evaluated using the confusion matrix, ROC curves and the parameters precision, recall, accuracy and f1 - score.

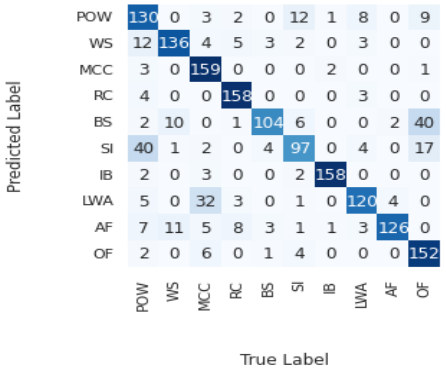

Figure 5: Confusion matrix with the *NSCNNMGeophysical* model with cut-off point at 0.5. Research source.

Table 5: Test with cutoff point at 0.5 with the TenGeoP-SARwv database. Research source.

	Precision	Recall	F1-score	Support
Pure ocean waves	0.98	0.96	0.97	165
Wind streaks	0.69	0.92	0.79	165
Micro convective cells	0.90	0.63	0.74	165
Rain cells	0.85	0.73	0.78	165
Biological slicks	0.86	0.82	0.84	165
Sea ice	0.95	0.76	0.85	165
Iceberg	0.74	0.96	0.84	165
Low wind areas	0.89	0.96	0.92	165
Atmospheric front	0.63	0.79	0.70	165
Oceanic front	0.78	0.59	0.67	165
Accuary			0.81	1650

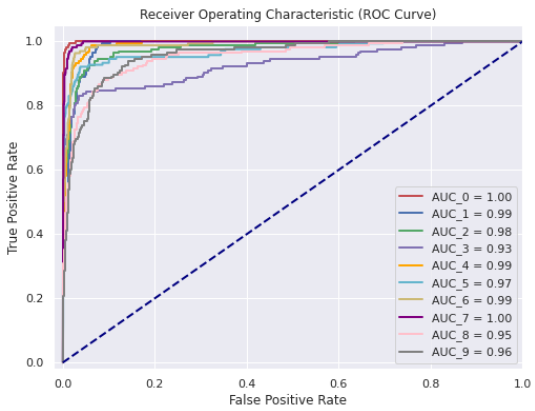

Figure 6: ROC curve of classes "POW":0, "WS":1, "MCC":2, "RC":3, "BS":4, "ST":5, "TB":6, "LWA":7, "AF":8 and "OF":9, Source: Research Imaging.

3. CONCLUSIONS

In this work, a new non-sequential neural network with parallel convolutional layers called NSCNNMGeophysical was proposed, this neural network classifies ten types of geophysical phenomena present in the TenGeoP-SARwv database, the neural network showed good results when evaluated with different types of performance metrics, achieving an area under the ROC curve greater than 0.9 for all classifications.

The model is able to detect anomalies present in the ocean, with this information we can have a better control of the maritime areas and thus prevent environmental or natural disasters. As future work we propose to improve the NSCNNMGeophysical model by increasing the recognition classes and thus complement a physical maritime control system.

4. REFERENCES

[1] H. Mc Nairn and B. Brisco, "The application of C-band polarimetric SAR for agriculture: A review," Can. J. Remote Sens., vol. 30, no. 3, pp. 525–542, 2004, doi: 10.5589/m03-069.

[2] G. Herrera, R. Tomás, J. López Sánchez, O. Monserrat, G. Cooksley, and J. Mulas de la Peña, "Sistemas radar aplicados a la investigación de subsidencia y movimientos de ladera," Enseñanza las ciencias la tierra, vol. 17, no. 3, pp. 316–324, 2009.

[3] J. P. J. Quintana, R. Moreno, "Estimation of flooded areas during the El Niño Costero 2017 event using multisensor satellite data. Case Study: Lower Piura watershed (Peru) | IEEE Conference Publication | IEEE Xplore." https://ieeexplore.ieee.org/abstract/document/9666917 (accessed Jan. 23, 2022).

[4] J. Fan, F. Zhang, D. Zhao, and J. Wang, "Oil Spill Monitoring Based on SAR Remote Sensing Imagery," Aquat. Procedia, vol. 3, pp. 112–118, 2015, doi: 10.1016/j.aqpro.2015.02.234.

[5] A. Colin et al., "Segmentation of Sentinel-1 SAR Images Over the Ocean, Preliminary Methods and Assessments," pp. 4067–4070, Oct. 2021, doi: 10.1109/IGARSS47720.2021.9553429.

[6] D. Masiliūnas, "Evaluating the Potential of Sentinel-2 and Landsat Image Time Series for Detecting Selective Logging in the Amazon," no. April, p. 54, 2017.

[7] R. Wiryadinata, M. Khoirussolih, N. Rohanah, I. Muttakin, and T. Firmansyah, "Image Data Acquisition for NOAA 18 and NOAA 19 Weather Satellites Using QFH Antenna and RTL-SDR," MATEC Web Conf., vol. 218, pp. 1–8, 2018, doi: 10.1051/matecconf/201821802002.

[8] United Nations, "Global indicator framework for the Sustainable Development Goals and targets of the 2030 Agenda for Sustainable Development Goals and targets", Inter-agency and Expert Group on SDG Indicators (IAEG-SDGs), March 2021.

[9] United Nations, "EO4SDG: EARTH OBSERVATIONS in Service of the 2030 Agenda for Sustainable Development". Earth Observations For Sustainable Development Goals Earth Observations For Sustainable Development Goals.

[10] C. Wang et al., "A labelled ocean SAR imagery dataset of ten geophysical phenomena from Sentinel-1 wave mode," Geosci. Data J., vol. 6, no. 2, pp. 105–115, Nov. 2019, doi: 10.1002/GDJ3.73.